Ferrimagnetism and abnormal spin–lattice coupling in dilute magnetic ferroelectric $(Bi_{0.46}Na_{0.46}Ba_{0.08})TiO_3$:Co*

Fan Jing(范 婧)[a)b)], Dong Xin-Wei(董新伟)[a)b)], Song You(宋 友)[a)], Wang Ke-Feng(王克锋)[a)b)], Liu Jun-Ming(刘俊明)[a)b)†], and Jiang Xiang-Ping(江向平)[c)]

[a)] *Laboratory of Solid State Microstructures, Nanjing University, Nanjing* 210093, *China*

[b)] *International Center for Materials Physics, Chinese Academy of Sciences, Shenyang* 110016, *China*

[c)] *Department of Material Science and Engineering, Jingdezhen Ceramic Institute, Jingdezhen* 333001, *China*

(Received 29 December 2009; revised manuscript received 18 June 2010)

We have investigated the low-temperature magnetism and spin–lattice coupling in $(Bi_{0.46}Na_{0.46}Ba_{0.08})TiO_3$:Co in order to understand the magnetoelectric effect in such artificially synthesized dilute magnetic ferroelectrics. It is revealed that the as-prepared $(Bi_{0.46}Na_{0.46}Ba_{0.08})TiO_3$:Co at Co content of 20%∼30% exhibits fascinating ferrimagnetism which is robust against magnetic field, the abnormal spin–lattice coupling characterized by a negative magnetostriction effect; and the suppressed magnetic moment within the temperature range of 30 K∼50 K is identified. These magnetic behaviours at low temperatures can be explained by the competition between the ferrimagnetic response and the magnetic moment suppression induced by the abnormal spin–lattice coupling effect. Finally, the ferroelectric and magnetodielectric properties are also discussed.

Keywords: ferrimagnetics, magnetostriction, ferroelectricity

PACS: 75.50.Gg, 75.30.Wx, 75.80.+q **DOI:** 10.1088/1674-1056/20/2/027502

1. Introduction

Magnetoelectric (ME) materials, in which a variation of electric polarization may be generated by external magnetic field and that of magnetization may be activated by external electric field, have drawn great attention due to their potential applications in emerging field of spintronics, data-storage media, and multiple-state memories.[1−7] Although the giant ME effect in piezoelectric–magnetostrictive composite ME materials has been extensively demonstrated,[8−11] people are still greatly concerned with single-phase ME compounds, partially because the ME compounds allow us to tune the ME effect in quantum-mechanical level, and partially for the high density integration with conventional integrated circuit (IC) technologies. So far, the most frequently investigated ME compounds are $Bi(Fe/Mn)O_3$ and rare-earth manganites with relatively small rare-earth ions, among which quite a number of perovskite oxide compounds were extensively addressed in recent few years.[1] Huge effort has been devoted to improving the ME effect in these single-phase compounds while it remains weak and often inaccessible for practical applications.

Besides the ME composites and single-phase compounds intensively addressed, there have been some additional attempts focusing on synthesizing artificial materials with considerable ME effect.[12−14] One of the possible approaches is to synthesize magnetic species doped ferroelectric materials in order to explore the possibility of synthesizing artificial materials with good ME performance. This approach is analogous to the strategy of synthesizing diluted magnetic semiconductor (DMS) in which magnetic doping into conventional semiconductors is done (such as ZnO:Mn(Co), Si:Mn(Co), etc.), for spintronics applications.[15,16] We may then call these ME materials dilute magnetic ferroelectrics (DMF). Along this line, two issues have to be addressed. One is to synthesize DMF materials and characterize their ME performances, and the ultimate goal is to obtain the high-quality ME materials for device utilization at above room temperature. Researchers are challenged by similar problems as taken in single-phase multiferroic compounds: How to develop a magnetic

*Project supported by the National Natural Science Foundation of China (Grant Nos. 50832002 and 10874075), the National Basic Research Program of China (Grant Nos. 2009CB613303 and 2009CB929501), and the Natural Science Foundation of Jiangsu Province, China (Grant No. BK2008024).

†Corresponding author. E-mail: liujm@nju.edu.cn

© 2011 Chinese Physical Society and IOP Publishing Ltd

order with high ordering temperature, while maintaining the original ferroelectric order in DMF materials, and consequently how to achieve a strong ME coupling. The other is to understand the microscopic origin of the ME performances, in particular the magnetic behaviour and spin–lattice coupling effect; the latter is the basis for understanding the ME coupling. Usually, as the first step, the spin configuration and spin–lattice interactions in these materials will be emphasized.

In the present work, we report our effort on the second issue in an artificially synthesized DMF material, while the first issue will be investigated too. For the material, we choose the recently concentrated ferroelectric solid solution, which is composed of 92% $(Bi_{1/2}Na_{1/2})TiO_3$ and 8% $BaTiO_3$, i.e. $(Bi_{0.46}Na_{0.46}Ba_{0.08})TiO_3$ (BNBT), and make Co-doping into BNBT, to synthesize DMF material BNBT:Co. It is known that BNBT has been considered as one of the promising and lead-free piezoelectrics due to its good piezoelectric performance and non-pollution for environments.[17] Its ferroelectricity has also been well documented in the literature.[18,19] Element Co and its oxides are traditional magnetic materials with affluent magnetic structures. Therefore, it is of interest to synthesize BNBT:Co compounds and investigate their magnetic configuration and spin–lattice interactions for potential ME applications, which have not been investigated so far. We not only focus on these properties at low temperatures (T), but also check the ferroelectric and ME properties, while more extensive ME performance over a broad temperature range will be reported in future. Interestingly, a ferrimagnetic (FIM) order at low T, robust to external magnetic field, is identified. For the spin–lattice coupling, an abnormal negative magnetostrictive effect within T-range of 30 K∼50 K is revealed, which results in a suppression of the FIM-aligned magnetic moment under magnetic field. We argue that the magnetic behaviour of BNBT:Co originates from the competition between the FIM order and abnormal spin–lattice coupling in response to external magnetic field. We also present preliminary experimental evidence that the as-prepared BNBT:Co maintains good ferroelectric property and exhibits remarkable ME effect at low T.

2. Experimental details

In our experiment, BNBT:Co with Co content (x) up to 30% was prepared by solid state reaction (details of the sample preparation are the same as in Ref. [18]). The sample crystallinity and microstructure were checked by x-ray diffraction (XRD) using Cu $K\alpha$ radiation and transmission electron microscopy (TEM) based on the standard ion-polishing processing of the samples. The x-ray photoelectron spectroscopy (XPS) was used to identify the valences of Co ions, with data collected after ion-polishing the sample surface. The binding energy (BE) data from the XPS spectrum were carefully calibrated referring to the C 1s peak after setting its BE to 284.6 eV.

The magnetic performance of the samples was characterized using superconducting quantum interference device (SQUID) and physical property measurement system (PPMS) (Quantum Design Inc). The zero-field-cooled (ZFC) data were collected by cooling samples under zero magnetic field down to $T = 2$ K and then measuring the magnetization under 1000 Oe (1 Oe=80 A/m) during the warming sequence. The field-cooled (FC) data were measured with the sample cooling under field H down to $T = 2$ K and the measuring field identical to H if $H < 1000$ Oe and equal to 1000 Oe if $H > 1000$ Oe. The magnetostriction coefficient λ of each sample as a function of magnetic field H, was probed using standard strain gauge method. In order to exclude the strain induced by thermal expansion of the sample at different T, we cooled the sample to a given T under $H = 0$ and performed careful calibration of the strain gauge indicator, then measured the sample strain as a function of H at this fixed temperature.

The ferroelectric hystereses at various T were measured using the standard RT6000 ferroelectric tester (Radiant Technologies, NM) under the virtual ground condition, with the sample being immersed into a temperature-controllable Dewar filled with liquid nitrogen. The dielectric property was evaluated using an HP4294A impedance attached to the sample in the PPMS system mentioned above. For data reliability, we used the same sample sets for these measurements, in order to exclude any uncertainties from sample to sample.

3. Results and discussion

3.1. Structural characterization

Our experiment demonstrates that the Co-doping into BNBT at a level as high as 30% does not change the single phase perovskite structure of BNBT. Pure BNBT is of a tetragonal structure with $P4mm$ lattice

symmetry. Figure 1(a) shows the measured XRD θ–2θ patterns for pure BNBT and four BNBT:Co samples with Co-contents x = 5%, 10%, 20% and 30% respectively. In respect of pure BNBT sample, the four BNBT:Co samples do show slightly rough spectrum background and broad reflections, however, no reflection from impurity phase is observed, in the high Co content of 5%∼30%. The broad reflections with relatively long tail indicate that the doping enhances the lattice inhomogeneity and induces random distortion of the lattice structure. Note that no indexing is possible for Co_2O_3, Co_3O_4.

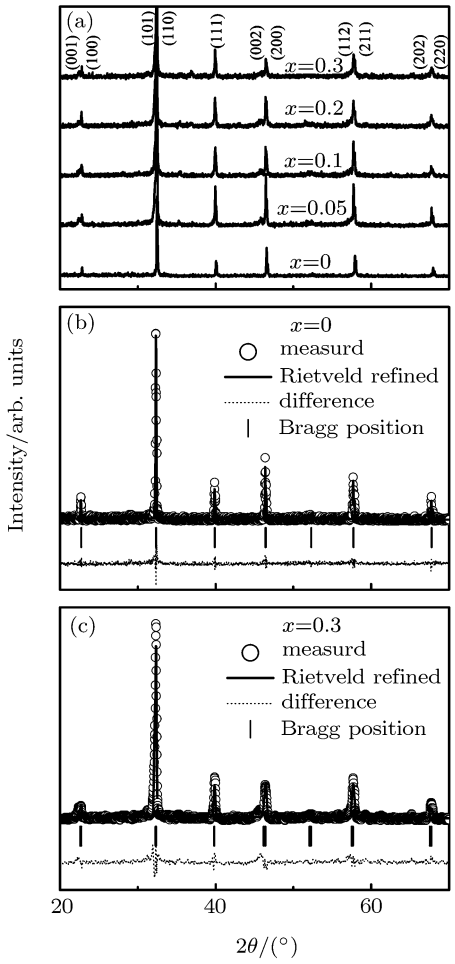


Fig. 1. (a) The x-ray θ–2θ diffraction patterns of BNBT, and BNBT:Co with x = 0.05, 0.1, 0.2, and 0.3, respectively. (b) and (c) The x-ray θ–2θ diffraction lines (open circles, measured) and evaluated ones (solids line, using Rietveld structural refinement) for sample BNBT and BNBT:Co with x=0.3, respectively. The difference (dot line, difference) between the measured and Rietveld refined lines for the two samples, respectively, is plotted with a slight downshift for clarity in (b) and (c). The short vertical solid lines, as guide for eyes, are the corresponding Bragg positions.

Additional evidence is obtained by performing the Rietveld refining of the measured XRD lines. Figures 1(b) and 1(c) show respectively the Rietveld refined data for two samples: pure BNBT and BNBT:Co (x=0.3), where the open circles represent the measured data, the solid lines are the Rietveld refined results, and the short vertical solid lines, as guide for eyes, are the corresponding Bragg reflection positions. Quite small difference between the measured reflections and refined ones is identified. For the other BNBT:Co samples, we obtained similar refined results. The reliability of the Rietveld refinement is demonstrated by the high-quality refinement parameters $R_{\rm wp}$ = 4.65% and 5.43% for the pure sample, and $R_{\rm p}$ = 3.51% and 3.62% for the x=0.3 sample. The calculated lattice parameters for pure BNBT sample are $a = b = 3.9042(6)$ Å (1 Å=0.1 nm), $c = 3.9085(1)$ Å, with a slight tension along the c axis with respect to the ideal cubic lattice. For the x=0.3 sample, one has $a = b = 3.9102(1)$ Å, $c = 3.9292(3)$ Å. It is rooted that the unit cell for the doped sample is larger than the pure one, and remarkable lattice tension along the c axis is observed. These facts may be explained by the bigger ionic radius of Co^{3+} (63 pm) than that of Ti^{4+} (60.5 pm).

Hereafter, we focus on characterization of the x=0.3 sample. We present further evidence on the tetragonal structure by performing TEM characterization. Figure 2(a) shows a low-magnification TEM image of the sample. It is clearly seen that the image contrast is quite homogeneous over the whole area, without identifiable second-phase particles. The high-resolution TEM image, in order to reveal the crystallinity and phase, is shown in Fig. 2(b), where the regular stripes in the (200) or (002) plane are clearly and homogeneously contrasted. The stripe spacing is 1.953 Å, consistent with the XRD data within the permission of uncertainties. In Fig. 2(c) is given the $[311]_P$ zone axis selected area electron diffraction (SAED) pattern. On one hand, the central spot is accompanied by a dim dispersing ring, indicating the effect of lattice deformation due to the Co doping (x=0.3 here). On the other hand, no SAED pattern from cobalt oxides has been observed.

It should be mentioned that no detailed knowledge on the site occupation of Co is available from our structural data. We believe that Co ions may mainly exist at the B site of BNBT, since the ionic radius of Co ion is very close to that of Ti ion. However, we have no intention to assign the Co ions in replacement of Ti ions, and the details of the Co ion occupancy in the lattice remains to be determined. We check the

chemical valence of Co ions using the XPS technique and the data are plotted in Fig. 3. Due to the spin–orbit coupling, the Co 2p core level is split into the $2p_{1/2}$ and $2p_{3/2}$ components. For the high-spin Co^{2+} state, a main peak at ∼780 eV with an intense satellite peak at ∼787 eV (as indicated by the arrow) should be observable, while the satellite intensity of the Co 2p for the Co^{3+} state is weak.[20−22] Figure 3 allows us to argue that the chemical valence of Co ions is Co^{3+} and no evidence of Co^{2+} is available.

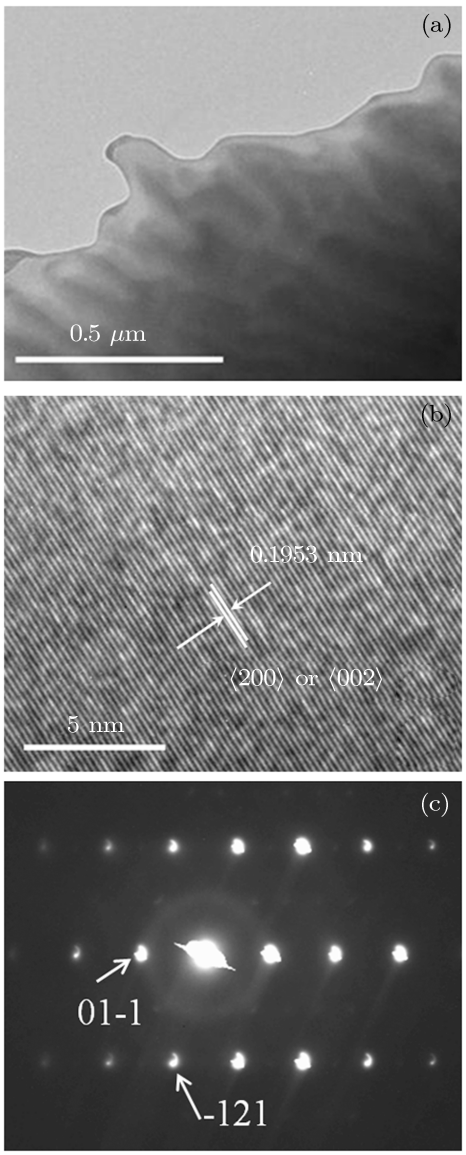


Fig. 2. (a) Low-magnification TEM image and (b) high-resolution TEM image of the BNBT:Co sample x=0.3. (c) The SAED pattern demonstrating the tetragonal symmetry of the structure. Note that the stripe-like contrast in (a) is due to the non-uniform thickness of the sample for TEM observation.

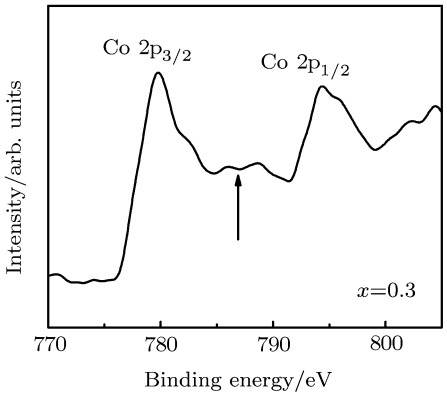


Fig. 3. The XPS spectrum of BNBT:Co sample with Co content of 30%.

3.2. Ferrimagnetic behaviours

We then look at the magnetic behaviour of the x=0.3 sample in low-T range, while the x=0.2 sample shows similar magnetic behaviours and magnetoelectric properties. Figure 4(a) shows the magnetization $M(T)$ under ZFC and FC (H = 1000 Oe) conditions.

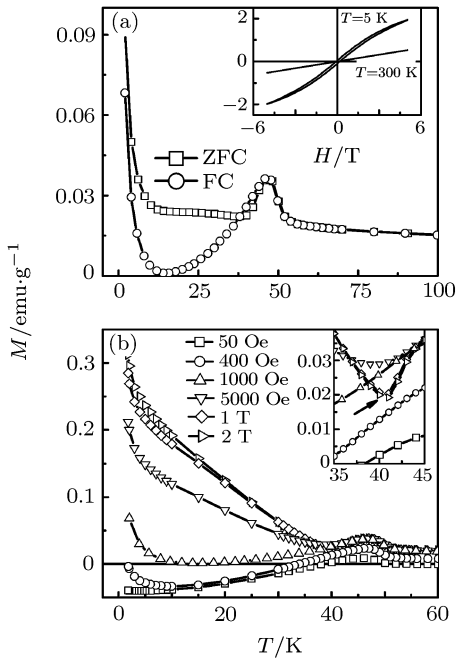


Fig. 4. (a) Measured magnetization M as a function of T under ZFC and FC conditions, and the inset shows the measured M–H hysteresis at 5 K and 300 K. (b) Measured M as a function of T under different cooling field H as labeled. The inset shows an enlargement of the data between 35 K and 45 K with the arrow indicating the magnetization suppression under the field of 1.0 T and 2.0 T respectively, with respect to the data under lower fields. All data are for BNBT:Co with x=0.3.

From the ZFC $M(T)$ data one sees a clear magnetic transition peaked at T = 50 K. This transition may

correspond to an antiferromagnetic (AFM) order below 50 K, as is likely confirmed by the very small moment and the negative intersection temperature using the Curie–Weiss formula fitting to the data over the high-T range. At extremely low T, the $M(T)$ exhibits somehow spin-glass-like behaviour, indirectly revealed by the unsaturated hysteresis loop at $T = 5$ K in the inset of Fig. 4(a). An unusual anomaly is observed that the FC $M(T)$ is remarkably smaller than the ZFC $M(T)$ over the whole T-range below 50 K, indicating that the magnetic order at $T < 50$ K must be ferrimagnetic (FIM) instead of AFM type. To further confirm this FIM order, we performed the $M(T)$ measurements under FC conditions with $H = 5$, 400, 1000, 5000, 10000 and 20000 Oe, respectively, and the data are plotted in Fig. 4(b). It is shown that the measured $M(T)$ over 5 K∼40 K at $H = 5$ Oe and 400 Oe is negative, a clear indicator of the FIM order within this T-range.

In fact, classical theory on ferrimagnetism predicts that magnetization can change its sign, i.e., the magnetic poles can invert at a particular temperature (so-called compensation point $T_{\rm comp}$).[23] Besides, the negative magnetization was observed in a number of FIM systems such as $NiFe_{2-x}V_xO_4$ and $(Fe^{II}_{0.40}Mn^{II}_{0.60})_{1.5}Cr^{III}(CN)_6$, etc.[24–26] For BNBT:Co investigated here, we argue that the two sublattices of spins in the FIM lattice may have different ordering temperatures ($T_{\rm m1}$ and $T_{\rm m2}$). The field cooling under small H (5 Oe and 400 Oe) drives the spin ordering of one sublattice with smaller moment along H at $T_{\rm m1}$, followed by the spin ordering of the other sublattice with larger moment which is antiparallel to H at $T_{\rm m2} < T_{\rm m1}$, leading to a negative magnetization below $T_{\rm m2}$. Such an argued physical picture is schematically illustrated in the lower part of Fig. 5(a) with $T_{\rm m2} < T_{\rm comp} < T_{\rm m1}$, while the upper part shows the measured M–T data under two different fields (5 Oe and 400 Oe). Furthermore, from Fig. 4(b) it is identified that the FIM order of the present BNBT:Co is robust against external magnetic field. Given an increasing H from 5 Oe to 5.0 T for the FC processing, although the measured $M(T)$ below $T = 35$ K reverses from negative to positive value and becomes almost saturated above $H = 1.0$ T, the saturated magnetic moment measured under $H = 2.0$ T at $T = 6$ K is only 0.0414 $\mu_{\rm B}$/Co, much smaller than the high spin moment of Co ion. This indicates that the spin order remains to be FIM under such high magnetic fields.

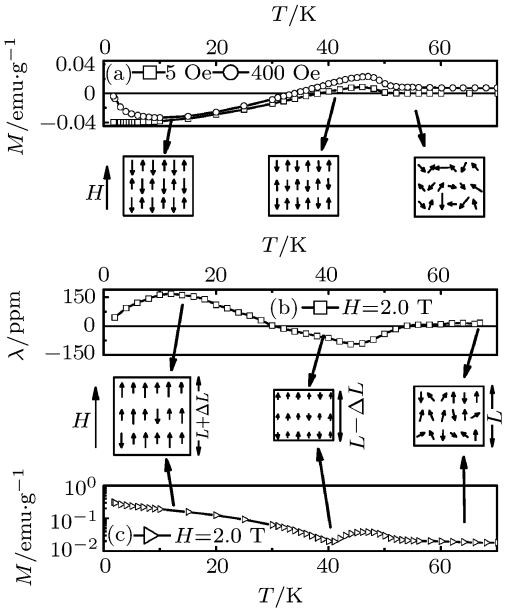


Fig. 5. (a) Measured $M(T)$ under cooling field $H = 5$ Oe and 400 Oe, respectively. The schematic spin lattices at several temperatures are inserted for illustration. (b) Measured $\lambda(T)$ under $H = 2$ T, and (c) measured $M(T)$ under cooling field $H = 2$ T. Possible spin lattices with corresponding lattice strain at several temperatures are schematically drawn for better illustration. These schematic illustrations are for guide of eye.

It should be mentioned here that the FIM order is not often observed in perovskite oxides although there have indeed been reported several perovskite oxides which exhibit the FIM order at low T. For example, the FIM order was identified in association with charge order in layered perovskite $GdBaMn_2O_5$,[27] and in Sr_2CrOsO_6,[28] both of which are perovskite compounds.

However, the measured FC $M(T)$ between 35 K∼50 K shows even more fascinating behaviour against H for the FC processing, as revealed in Fig. 4(b), which is unusual for a FIM ordered system. This predicts the existence of an additional effect in competition with the magnetization process induced by the field cooling under various H. We replot the $M(T)$ data within 35 K∼45 K, as shown in the inset of Fig. 4(b). Looking at the data at $T = 40$ K, as an example, one finds that M increases with H before reaching its maximum (0.03 emu/g) at $H \sim 5000$ Oe, and afterwards M falls down to 0.02 emu/g at $H \sim 1.0$ T and above. Note that the relative variation of the moment is remarkable. This behaviour cannot be explained only by the FIM order and its response to the large external field.

3.3. Spin-lattice coupling

We then investigate the spin–lattice coupling in the BNBT:Co sample, which induces the lattice expansion or contraction under a magnetic field. This coupling is found to influence the magnetization behaviour at $T < 50$ K and magnetization suppression between 35 K∼50 K. Figure 6(a) shows the measured strain λ (ppm) at different T as a function of H. It is clearly revealed that $\lambda(H)$ behaves in an approximately parabolic form at low H and then tends to be saturated at high H, indicating that the strain does originate from the magnetostriction. More importantly, it was observed that λ is negative between 30 K$< T <$50 K, while it becomes positive at $T < 30$ K and $T > 50$ K. For a clearer presentation, figure 6(b) plots the measured λ at $H = 2.0$ T as a function of T. Note that it is reasonable to observe small λ both above the FIM transition point (paramagnetic state) and $T \to 0$. This abnormal magnetostriction behaviour represents the complicated spin–lattice coupling in BNBT:Co, the details of which remain to be an issue worthy of careful investigation but unfortunately not fully available to us at this moment.

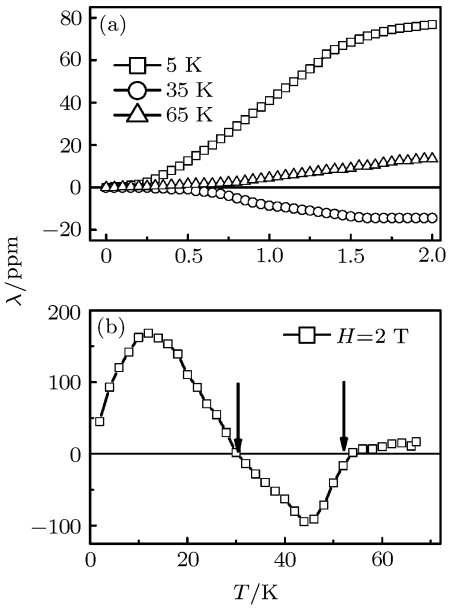


Fig. 6. Measured strain λ as a function of H at several temperatures (a) and as a function of T under $H = 2$ T. All data are for BNBT:Co with x=0.3.

The negative magnetostriction in cobalt oxides is not an unusual effect. Actually, as early as in 1968, a negative magnetostriction effect was predicated in AFM ordered cobalt oxide systems, which was due to the spin–orbital coupling associated with lattice distortion.[29] For the present BNBT:Co, at $T < 50$ K the Co^{3+} spins do align in the FIM order, consistent with this prediction, although the FIM order is slightly different from the AFM order. Nevertheless, the magnetostriction in an AFM Co^{3+} system is not necessarily negative, as revealed for the present BNBT:Co sample and other Co oxides.[30] As to the relationship between the magnetostriction and magnetization for BNBT:Co, one observes that the negative magnetostriction does correspond to the suppressed magnetization M. For an AFM (or FIM) ordered system, an external magnetic field as high as several Tesla cannot be responsible for the suppression of M, and instead, such a high field would enhance M if the FIM order could be melted by the applied field. However, it was revealed above (Fig. 4) that the low-T magnetization under a field of several Tesla does not change much due to the high robustness of the FIM order.

The only and also reasonable possibility available to us is that the reduction of magnetic moment between 35 K and 50 K occurs via the possible spin-crossover effect induced by the volume contraction, due to the negative λ in this T-range. We argue that for the present BNBT:Co, the negative magnetostriction likely enforces a spin-crossover of some Co^{3+} spins from the high-spin state $S = 2$ to low-spin state $S = 0$, which partially suppresses magnetization M. For Co^{3+}-oxides such as $LaCoO_3$, $SrCoO_3$, $Sr_2Co_2O_3$ and $Co(H_2(fsa)_2en)(py)_2$, etc., the spin-crossover represents a common phenomenon,[31] which can be controlled by external stimulation such as temperature, light-irradiation, magnetic field, and compressive pressure.[32] Recent theoretical modeling based on *ab initio* study and Monte Carlo method, plus delicate experiments, revealed that the external pressure-induced elastic compression, caused by lattice distortion due to the molecular size difference between the high-spin and low-spin states, can induce the spin-crossover.[33] While usual external magnetic field should favour a spin-crossover of Co^{3+} spin from the low-spin state S=0 to the high spin state S=2, i.e. field enhanced magnetization, here for BNBT:Co the abnormal spin–lattice coupling with negative λ between 30 K and 35 K seems to result in the reverse process. This reverse process may be slightly superior to the field-enhanced magnetization; however we do not have direct and microscopic evidence to support this argument, and more details by utilizing neutron scattering are open for future work.

We illustrate once more this argued competition by the sequence highlighted in Figs. 5(a) to 5(c), where

the possible two-sublattice spin configurations at different T are given schematically. In Fig. 5(a) is drawn the FIM ordering sequence with decreasing T and the corresponding magnetization $M(T)$. The present BNBT:Co sample is paramagnetic at $T > 50$ K. At $T \sim 50$ K, the spins in the first sublattice begin to show the FM ordering and align along H. With decreasing T, the spins in the second sublattice align ferromagnetically but in opposite to the spins in the first sublattice, leading to the transition of M from $M > 0$ to $M < 0$. We replot in Fig. 5(b) the strain λ as a function of T together with the possible spin configurations at different T. Some Co^{3+} spins favour the low-spin state between 30 K and 50 K, due to the field-induced negative magnetostriction, while most Co^{3+} spins may remain unchanged in the high spin state. In Fig. 5(c) we plot the resultant M as a function of T due to the competition between the FIM ordering and the abnormal spin–lattice coupling in response to external field H.

3.4. Ferroelectricity and magnetodielectric effect

Finally, as an evidence to support the original motivation for DMF materials, we present the measured data of the ferroelectricity and magnetodielectric effect. While it is well known that a magnetic doping into ferroelectrics usually damages seriously the electric property, we demonstrate that the ferroelectricity in the present BNBT:Co sample remains good. The measured hysteresis loops at different temperatures are plotted in Fig. 7(b), while the loops for pure BNBT are shown in Fig. 7(a). It is seen that at ~ 300 K and ~ 200 K, both BNBT and BNBT:Co exhibit high-quality ferroelectric hysteresis. As T is lowered down to ~ 100 K, the measured loops are far from saturated due to the fact that the coercive field becomes too high to be accessible at low T, in our experiment.

However, we can access the magnetodielectric property at much lower T in order to see the ME effect, although the magnetodielectric (MC) effect is not necessarily equivalent to the ME effect. Figure 8 shows the measured MC ratio ($\Delta\varepsilon(H) = (\varepsilon(H) - \varepsilon(0))/\varepsilon(0)$) of the BNBT:Co sample as a function of T at three frequencies of the AC signal, where ε is the dielectric constant and H is magnetic field. While no MC effect is observed for pure BNBT, the BNBT:Co sample exhibits clear dielectric response to magnetic field, although this response is not significant and usually true for those typical multiferroic compounds. What is interesting here is that the T-dependence of $\Delta\varepsilon(T)$ shows an anomaly at $T \sim 50$ K, at which the FIM ordering ensues. The measured $\Delta\varepsilon$ below 50 K is much higher than that above 50 K. The MC effect and the anomaly at the FIM ordering point indicate the existence of the spin–dipole coupling in the present BNBT:Co. In fact, such coupling and the anomaly near the FIM/AFM ordering point are the ingredient of the ME effect and were observed in many geometrically frustrated magnets.[34]

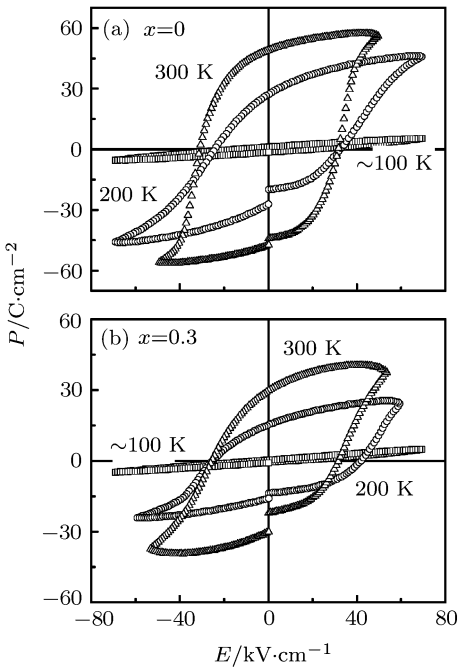


Fig. 7. Measured ferroelectric hysteresis loops for BNBT (a) and BNBT:Co with x=0.3 (b) at $T =\sim 100$, 200, and 300 K.

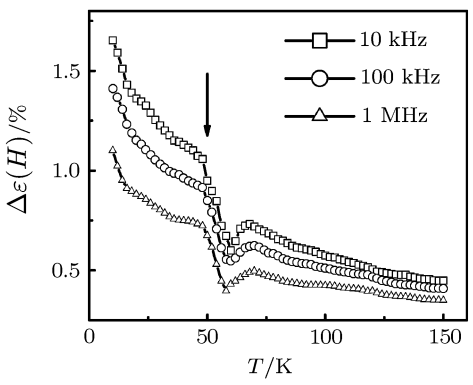


Fig. 8. Measured magnetodielectric ratio as a function of T under $H = 5$ T with the measuring frequency from 10 kHz to 1 MHz. All data are for BNBT:Co with x=0.3.

4. Remarks and conclusion

It should be remarked here that the present work mainly deals with the magnetic behaviours and spin–lattice coupling in the low-T range. Although we also investigated the electrical properties of the BNBT:Co materials, such as ferroelectricity and magnetodielectric behaviours, no details of the ME coupling and the associated physics have been addressed. It seems that the Co doping into BNBT does lead to formation of magnetically ordered structure, which is a prerequisite for an ME material. The strong and anomalous spin–lattice coupling has been identified. However, the measured ME effect has been so far insufficient as expected, while the ferroelectricity remains quite good. We believe that the present protocol for DMF synthesis represents a promising approach to novel materials for ME applications, upon significant enhancement of the ME effect and profound understanding of the physics associated with the high-T magnetic ordering, strong spin–lattice coupling, and thus remarked ME effect.

In summary, we have successfully prepared single-phase DMF materials BNBT:Co with Co^{3+} content up to 30%, and then investigated in details the low-T magnetism and spin–lattice coupling effect. It has been demonstrated that the Co-doping does not change the tetragonal structure of BNBT. The BNBT:Co material exhibits ferrimagnetism and abnormal spin–lattice coupling behaviours below 50 K. The ferrimagnetic state is robust against external magnetic field and cannot be melted under a field of several Tesla. We have observed a partial suppression of the magnetization by magnetic field between 35 K and 50 K, which is argued to originate from the competition between the ferrimagnetic ordering and abnormal spin–lattice coupling. Finally, the ferroelectricity and magnetodielectric effect of the BNBT:Co materials have been discussed. The present work sheds some light on the rich physics associated with DMF oxides.

References

[1] Wang K F, Liu J M and Ren Z F 2009 *Adv. Phys.* **58** 321
[2] Eerenstein W, Mathur N D and Scott J F 2006 *Nature* **442** 759
[3] Cheong S W and Mostovoy M 2007 *Nature Mater.* **6** 13
[4] Ramesh R and Spaldin N A 2007 *Nature Mater.* **6** 21
[5] Fiebig M, Lottermoser Th, Fröhlich D, Golsev A V and Pisarev R V 2002 *Nature* **419** 819
[6] Ge B H, Li F H, Li X M, Wang Y M, Chi Z H and Jin C Q 2008 *Chin. Phys.* B **17** 3163
[7] Xu F, Bai Y, Ai F and Qiao L J 2008 *Chin. Phys.* B **17** 4652
[8] Zhang Y, Deng C Y, Ma J, Lin Y H and Nan C W 2008 *Chin. Phys.* B **17** 3910
[9] Petrov V M, Srinivasan G and Laletsin U 2007 *Phys. Rev.* B **75** 174422
[10] Thiele C, Dörr K, Bilani O, Rödel J and Schultz L 2007 *Phys. Rev.* B **75** 054408
[11] Lin Y H, Cai N, Zhai J Y, Liu G and Nan C W 2005 *Phys. Rev.* B **72** 012405
[12] Dong X W, Wu Y J, Wan J G, Wei T, Zhang Z H, Chen S, Yu H and Liu J M 2008 *J. Phys.* D: *Appl. Phys.* **41** 035003
[13] Nénert G and Palstra T T M 2007 *Phys. Rev.* B **76** 024415
[14] Nugroho A A, Bellido N, Adem U, Nénert G, Simon C, Tjia M O, Mostovoy M and Palstra T T M 2007 *Phys. Rev.* B **75** 174435
[15] Oshio T, Masuko K, Ashida A, Yoshimura T and Fujimura N 2008 *J. Appl. Phys.* **103** 093717
[16] Passacantando M, Ottaviano L, Orazio F D and Lucari F 2006 *Phys. Rev.* B **73** 195207
[17] Takenaka T, Maruyama K and Sakata K 1991 *Jpn. J. Appl. Phys.* **30** (Part I) 2236
[18] Jiang X P, Zhen Y Y, Jiang F L, Liu L H, Guo J R and Chan H L W 2007 *Chin. Phys. Lett.* **24** 3257
[19] Wang X X, Chan H L W and Choy C L 2005 *Appl. Phys.* A **80** 333
[20] van Elp J, Wieland J L, Eskes H, Kuiper P, Sawatzky G A, de Groot F M F and Turner T S 1991 *Phys. Rev.* B **44** 6090
[21] De Groot F M F, Abbate M, van Elp J, Sawatzky G A, Ma Y J, Chen C T and Setter F 1993 *J. Phys.: Condens. Matt.* **5** 2277
[22] Mizokawa T, Tjeng L H, Steeneken P G, Brookes N B, Tsukada I, Yamamoto T and Uchinokura K 2001 *Phys. Rev.* B **64** 115104
[23] Néel L 1948 *Ann. Phys.* (Leipzig) **3** 137
[24] Fishman R S and Reboredo F A 2007 *Phys. Rev. Lett.* **99** 217203
[25] Zhang S X, Tan S, Tong W and Zhang Y H 2005 *Phys. Rev.* B **72** 014453
[26] Ohkoshi S I, Abe Y, Fujishima A and Hashimoto K 1999 *Phys. Rev. Lett.* **82** 1285
[27] Taskin A A and Ando Y 2007 *Phys. Rev. Lett.* **98** 207201
[28] Krockenberger Y, Mogare K, Reehuis M, Tovar M, Jansen M, Vaitheeswaran G, Kanchana V, Bultmark F, Delin A, Wilhelm F, Rogalev A, Winkler A and Alff L 2007 *Phys. Rev.* B **75** 020404
[29] Goodenough J B 1968 *Phys. Rev.* **171** 466
[30] Qiu J J, Han G C, Li K B, Liu Z Y and Zong B Y 2006 *J. Appl. Phys.* **99** 094304
[31] Bousseksou A, Boukheddaden K, Goiran M, Consejo C, Boillot M L and Tuchagues J P 2002 *Phys. Rev.* B **65** 172412
[32] Nishino M, Boukheddaden K, Konishi Y and Miyashita S 2007 *Phys. Rev. Lett.* **98** 247203
[33] Ding Y, Haskel D, Ovchinnikov S G, Tseng Y C, Orlov Y S, Lang J C and Mao H K 2008 *Phys. Rev. Lett.* **100** 045508
[34] Katsufuji T and Takagi H 2004 *Phys. Rev.* B **69** 064422